<u>Executive Summary and Business Analysis</u>

Breaking the Law: The Next Revolution in Computation through Optics

Ben Grau *University of Pennsylvania Electrical and Systems Engineering*
Justin Qian *University of Pennsylvania Material Science Engineering*
Sohum Daftary *University of Pennsylvania Electrical and Systems Engineering, Wharton*

In our lifetime, we have seen computers shrink from the size of a classroom desk to something that can fit on our wrists. Our parents' generation witnessed the transition from vacuum tubes that took up a building and were operated by teams of engineers to a sleek, yet ugly, TI-84 "pocket-sized" calculator. It was once a pipedream to think that normal people could own machines capable of solving their math homework in a matter of milliseconds. Imagine what college students of the '70s would say if we told them that one day, they'd be able to find a date, order a pizza, watch *Happy Days*, and listen to Pink Floyd, all simultaneously, on a device in the palm of their hands. They would have handed us a joint and replied with, "Far out, dude," ….or whatever people from the '70s used to say.

We've come quite a long way from the early days of the computer, but we're dreamers not historians. We wonder about our kids and future generations of students, professionals, entertainers, and everything in between. The limits of technological improvement on state-of-the-art computer chip technology are being realized due to limits in transistor-based manufacturing. The next generation will find it difficult to unlock the future of their technological potential because the size of the computer chip cannot be scaled down further. We have developed a new chip that uses light and lenses to make computations faster and on a substantially smaller scale, giving future people the same thrill of leaps in technology that we experienced.

In various technological domains from Big Data to artificial intelligence, the demand for computation and need for scale in computation has increased quickly. Unfortunately, innovation in the transistor space has been primarily incremental with improvements in chip density, parallel processing, and chip sizing using marginally more expensive fabrication techniques. Our chip uses a metasurface, a collection of nanoscale shapes of different materials, to create a lens that can take data-bearing light and perform mathematical operations on it. Thus, we complement the transistor in computation.

Our system provides a complement to purely electronic architectures by increasing the speed of data transfer and processing while decreasing the size of devices and power consumed. Everyday users would be able to play PlayStation4 quality games on their Apple Watch without having the re-charge five times a day and taking a second mortgage on their house. Commercial cloud providers like Amazon could find substantial savings with scalable optoelectronic components and not need billions in tax subsidies from angry New Yorkers Breaking the barriers in size, speed, and power provides fundamental changes for computing technologies.

An optics based architecture can be integrated into the existing value chain for computer chips. The key elements of the chip value chain begin with the design tools and the materials, which have converged to photolithography, deposition, and silicon-based devices. Other frequently used materials include gold conductors and silicon dioxide insulators. Fabrication equipment used to support the beginning of the chip value chain has been fairly standardized in terms of etchers and depositors as well as characterization equipment. At the end of the value chain, device logic which builds applications for user is also standardized. Our device provides a new link between the beginning and end of the existing value chain by replacing the current architecture without requiring new fabrication tools or electronic systems and applications.

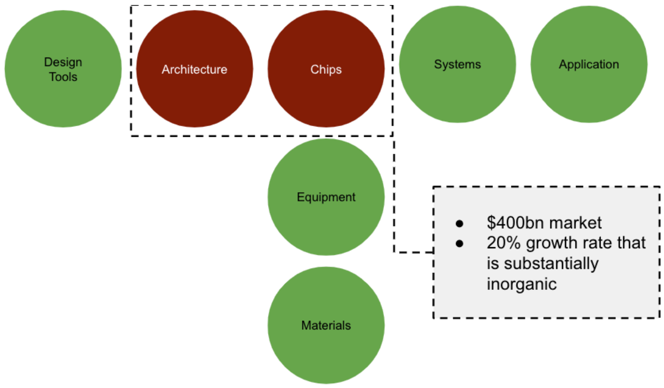

The target element of the value chain, comprised of the transistor and semiconductor industries, is worth over $400bn globally and is a growing industry that is fairly cyclical as demand is originated at the pace of economic development. Additionally, among the large chip manufacturers like TI and Intel, there has been a 20% increase in R&D spending and that R&D is substantially fueled by buying technology and talent that has the potential to advance current chip architectures.

Our customer is precisely the incumbent chip manufacturers, to whom we license the optoelectronic chip technology. Our fabrication process recognizes the reality of the fabrication ecosystem as well as the trend in “fabless” production where semiconductor firms outsource manufacturing to a standardized facility. The “plug-and-play” nature of our technology enables direct integration and combines process engineering with device innovation to fit the market.

Our competition begins with the status quo, transistor based technology (TI, Intel, TSMC,) that has reached a ceiling. Quantum architectures (Cambridge Quantum, D-Wave, and 1Qbit) are alternatives for supercomputing, yet they lack integration with status quo algorithms (see above graph) and need new ways of interacting with current application, posing substantial challenges. Optical computing companies (Optalysys, Nanosys, and Nano-Meta) do not use the metamaterial approach in chip design. They instead use optics for isolated applications like data transfer rather than replacing current architectures and maximizing the process integration with semiconductor manufacturing technologies.

Lastly, and being maybe too realistic, the majority of our revenues will be realized after a three to five year runway, during which the device will be shown to surpass the most cutting-edge transistor technologies. Based on the market size and taking a slice of .5% each year, we estimate revenues of $2bn starting in 2023. By 2030, we expect this number to grow to $20 bn. This is a conservative estimate that accounts for greedy competitors eating into our market share. Our costs will primarily be facilities and materials usage, which we expect to cost about $100mm each year on average based on our current usage and recognition of loss of academic discounts, and personnel, which will be a team of salaried researchers that the market pays about $200,000 per person per year, with about a 10 person team.

Metasurfaces for Analog Optical Signal Processing

S. Daftary, B.Grau, J. Qian
Advisors: Liang Feng & Nader Engheta

Abstract

Optical computation increases computation power over semiconductor devices by providing a higher bandwidth and potentially analog processing platform, as well as lower power consumption in computation. However, conventional optical components, which rely on gradual phase shifts, are unsuitable for an integrated circuit environment where size of the component and compatibility with complementary metal-oxide-semiconductor (CMOS) fabrication are important. In this work, we use ultrathin nanoantenna arrays to manipulate the phase profile of an incoming wave and perform mathematical operations on an incident optical signal. We demonstrate the ability of the metasurface to shape wavefronts by performing the Fourier transform on the optical signal; a capacity that can be extended by performing spatial filtering. In doing so, we implement the functionality of a traditional macroscale optical lens on the nanoscale.

Project Objectives

Computation power over the past several decades has grown rapidly as semiconductor companies have continued to scale down the size of CMOS transistors and optimize system architectures. However, current semiconductor technology faces the end of this scaling ability, as physical limits on the size of CMOS transistors are reached. Optical components, such as our metasurface, address computational limits in several ways and will continue the trend of increased computation power and speed that has fueled the modern electronic revolution.

Using an optical signal enables faster processing, via a higher bandwidth and the use of multiple frequencies that do not cross-talk to transmit information, than current CMOS processors that are clock speed-limited by the size of the transistors. Higher bandwidth operation enables quicker computation as many more operations per second can be completed. Furthermore, our metasurface can directly process the optical signal passed in. Directly tailoring the signal is advantageous as the signal can be processed quicker in this analog mode than by converting the signal into a digital signal and then performing many small operations on the bits that carry the signal's information. The metasurface approach is also preferred over traditional analog computation, where lumped circuit elements and bulky optical components are used, since the metasurface is passive (requiring no input energy), compact, and integrable on-chip.

Outside of computing applications, a deeply-subwavelength metasurface (meaning thickness much less than that of the wavelength of the incident wavelength) that can manipulate an incident optical signal has applications in, for example, cloaking, anti-reflection surfaces, and analog image recognition. Applications such as automatic feature detection in cameras or improvements in edge and boundary detections for robots or self-driving cars may potentially be improved with the use of such analog image processing. Furthermore, metasurfaces as lenses have applications outside photonics itself, being applicable where manipulation of light on the nanoscale is necessary, such as in quantum information platforms[1] and in imaging of nanoscale condensed matter physics systems[2]

Recent progress has also been made in using metasurfaces to focus light for nanoscale biomedical sensing applications, where femto-molar concentrations of substances can be detected in small sample sized[3] and very recently, to solve equations (perform an integration) in an analog fashion[4].

Our work more closely resembles the latter in a more tunable, albeit less efficient manner. Instead of fabricating the structures to perform a specific operation, however, we use a metasurface to perform the Fourier transform on an incident optical signal, allowing for a response which is tailorable, dependent on filtering at the focal point of the nanoscale lens.

Impact

In domains from Big Data to artificial intelligence, the demand for computation and need for scale in computation have risen quickly. For the Internet of Things, for example, an increase of 20-30 billion connected devices is expected by 2020[5]. The increase in devices and complexity of tasks, as well as the data produced by these devices, will require computation engines that can perform faster and on a smaller scale - all with less power consumption. Unfortunately, innovation in the transistor space has been primarily incremental with improvements in chip density, parallel processing, and chip sizing using more expensive fabrication techniques. Disruptive innovation that changes the architecture of computational systems is necessary to keep up with the pace of computational demand. Optical systems provide a complement to purely electronic architectures by increasing the rate of data transfer and processing while potentially decreasing the size of devices and power[6]. For an end consumer, devices would have higher quality graphics, more portable computation engines, and longer battery life. For commercial cloud providers, this means substantial savings to scalable optoelectronic components. Large server farms and high-performance computing centers house thousands of parallel cores where each additional core or unit comes at an increasing marginal cost with decreasing marginal benefit due to power and maintenance limits of modern computers[7]. Additionally, even profitable centers face communication issues that optics has already started resolving. Moving data between units after processing can be performed more efficiently using light, traditionally under the fiber optics domain[8]. With optical configurations and the ability to quickly compute the Fourier transform of a light signal, the data transfer can include filtering and cleaning mechanisms in addition to the communication function. Lastly, with large and small firms using cloud services and edge computing to outsource processing, faster and scalable optoelectronics can provide cost savings to certain firms that elect to keep processing in house by offering an energy efficient and high-performance alternative.

We seek to build a device at the nanoscale that replicates the essential functions of a lens. The device will be a combination of various materials and surfaces (metasurface) that together mold a wavefront for an incoming visible or infrared light wave and produce a focal point. In addition to the device, we will provide simulation results of scatters that further our understanding of light propagation through subwavelength features. Test results comparing the simulation and the device will also be delivered in order to understand the quality of the device and the manufacturing process. Taken together, the device, tests, and simulation will also produce helpful information about the applicability and viability of alternative computing architectures.

An optics based architecture can be integrated into the existing value chain for computer chips without creating substantial disruption. The key elements of the chip value chain begin with the design tools and the materials, which have converged to photolithography, deposition, and silicon-based devices. Other frequently used materials include gold conductors and silicon dioxide insulators. Fabrication equipment used to support the beginning of the chip value chain has been fairly standardized in terms of etchers and depositors as well as characterization equipment. At the end of the value chain, device logic which builds applications for user is also standardized. Our device provides a new link between the beginning and end of the existing value chain by replacing the current architecture without requiring new fabrication tools or electronic systems and applications[9]. The target element of the value chain, comprised of the transistor and semiconductor industries, is worth over $400bn globally[10] and is a growing industry that is fairly cyclical as demand is originated at the pace of economic development. The long-term impact of an optoelectronic device is to complement the current architecture in the most common cases, and thus, the value of the chip architecture market would grow as new market participants can combine rather than replace incumbents in advancing computing technology. Given that the latest findings from McKinsey indicate a 20% increase in R&D spend from the largest incumbents in the semiconductor market and that R&D is substantially fueled by buying technology and talent to obtain the latest edge, the device, if shown to perform, will most likely be integrated into the portfolio of a large fabricator rather than being manufactured as a standalone product[11]. To achieve our venture goal of being integrated into the macro-chip architecture industry, our fabrication process recognizes the reality of the fabrication ecosystem as well as the trend in fabless production where semiconductor firms outsource manufacturing to a standardized facility and attempts to use the most common fabrication procedures rather than developing new methodologies. In this way, we combine process engineering with device innovation to fit the market.

Project Methods

Design

The operation of interest is the Fourier transform, which arises naturally when considering many optical systems. For example, in the case of a thin convex lens (focal length = f) with some suitably small transmissive input placed a distance d front of the lens, the field in the focal plane is given by:

$$U_{output}(u,v) = \frac{A\exp\left(j\frac{k}{2f}\left(1-\frac{d}{f}\right)(u^2+v^2)\right)}{j\lambda f} \iint U_{input}(x,y)\exp\left(-j\frac{2\pi}{\lambda f}(xu+yv)\right)dxdy \tag{1}$$

Thus the field in the back focal plane is proportional to the Fourier transform of the incident field, and when $d = f$ the field in the back focal plane is the exact Fourier transform of the incident field. As mentioned earlier, lenses are bulky and difficult to fabricate in the near IR region due to limited materials choice, so it is desirable to use subwavelength plasmonic scatterer-based metasurfaces to produce the same effect at the nanoscale.

An ordinary lens induces a position dependent phase delay by modifying the path length of the incident light. The phase profile of a lens with focal length f is given by:

$$\varphi_L(x,y) = \frac{2\pi}{\lambda}\sqrt{x^2+y^2+f^2} - f \tag{2}$$

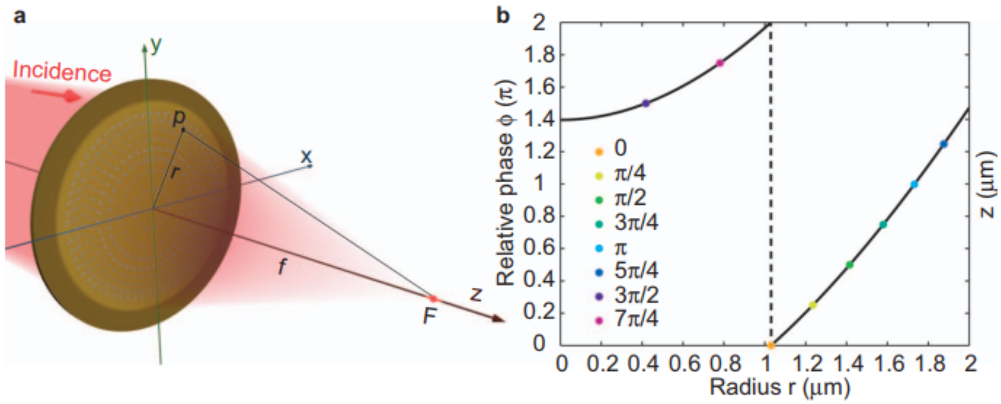

Figure 1[12] (a) Schematic of a lens. (b) Black line: optical phase shift profile desired to produce lensing effect. Colored points: eight discrete points used to approximate the desired phase response

Optical scatterers produce lensing behavior on a small scale by inducing optical phase discontinuities. These phase jumps can then be used as discrete points to approximate the desired phase profile, producing a lensing effect. For creating lenses with a tunable focal length, it is particularly critical to have full control over the phase from 0 to 2π. A simple metallic rod antenna (Figure 2a) is a plasmonic scatterer able to obtain a relatively large phase coverage by changing orientation and length, but the amplitude of the scattered light varies drastically with the phase shift. Plasmonic V-shaped antennas are our current candidate for optical element of choice. These antennas support a symmetric and antisymmetric mode that are excited to a different degree by incoming light, which allows for the polarization of the incoming light to be shifted. Furthermore, modifying the size and the shape of the antenna allows for control over the phase and amplitude of the shifted light. Thus unlike straight rod antennas, the phase coverage of the cross-polarized component of light for V-shaped antennas can be extended to the full range of 0 to 2π, while maintaining relatively constant amplitude (Figure 2c-d).

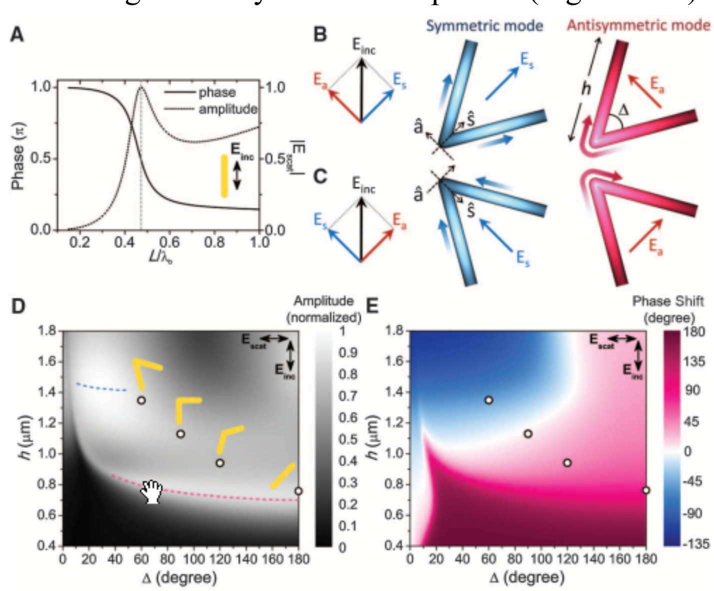

Figure 2[13] (a) phase and amplitude of scattered light from straight antenna. (b) symmetric and antisymmetric mode of V-shaped resonator. (d) amplitude

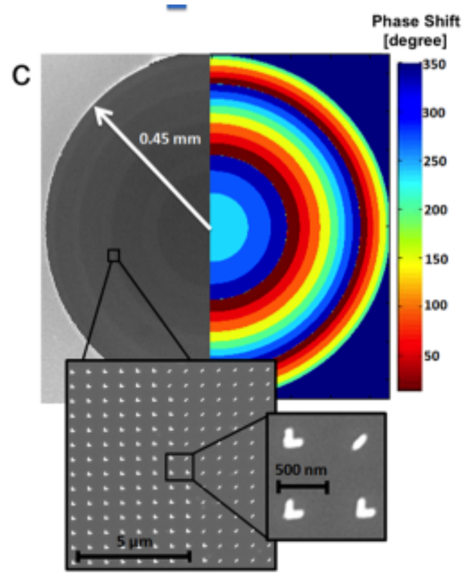

Figure 3[14] (c) right: desire phase shift profile of lens. Left: SEM images of patterned antennas used to achieve phase shift and (e) phase of scattered light corresponding to V-shaped scatterers with varying parameters.

After obtaining parameters for scatters with a suitable phase delay, they can be patterned on the substrate, separated by sub-wavelength distances (Figure 3c). The resulting lens is applicable for a range of wavelengths due to the broad resonance of the V-shaped antenna, however it is not achromatic due to the linear response of the phase to wavelength. The largest drawback is that the efficiency of these lenses is often quite low, around 1-10%. Careful control over the impedance and spacing of the scatterers will allow for improvements in efficiency. Furthermore, the Q-factor of commonly used plasmonic materials such as gold or silver, is quite low, leading to high losses, so a careful choice of material for a given wavelength may lead to efficiency improvements as well.

Results

Simulation

After thoroughly reviewing the literature and deciding on V-shaped antennas with varying lengths and central angles as our scatterer design, we began the simulation phase of our project. We decided to numerically analyze the scattering design using MATLAB and Python based on a mathematical approach found in the literature. With an input antenna length and angle of the V-shape, and given an incident electric field, we were able to calculate the plasmonically-induced current in the rod, for both antisymmetric and symmetric resonance modes. In principle, we can find the current density at any point along the rod, and then use the Green's function approach with integration along the rod to find the far-field phase of the electric field, which is our parameter of interest given the goal of tuning a 0 to 2π phase delay to replicate the function of a lens.

This analytical approach did not yield useful phase information for the scatters we wish to fabricate, since the calculation in Python or MATLAB does not account for various non-idealities in the system. Such non-idealities include the shape of the antenna rods, which we assumed to be cylindrical but in practice will be rectangular given our planned fabrication approach, and the conformality of and defects on the metal surface, as field effects are largely dictated by the smoothness and purity of the surface for a metallic conductor. Nonetheless, we gleaned some useful information from the analysis. Through our work, we have better understood the complex relationships among the polarization of the incident electric field, the shape of the antennas, both lengthwise and regarding angle, and the far field phase of the electric field.

The next step was to run full-wave three-dimensional simulations of individual scatterers using the wave optics module of COMSOL Multiphysics. A physical model for an ideal gold scatterer on a silicon substrate was built, and parametrized around arm length l, arm thickness t, height h, and arm angle θ. The goal of the simulation was to obtain the scattered cross-polarized field, which we refer to as $E_{scat,\,y}$, given some incoming $E_{inc,\,x}$ field propagating in the +z direction. The polarization of the incoming field (x) is shown in Figure 2b, and is defined so that it bisects the symmetric and antisymmetric mode, and is capable of exciting both. The model first solves for the total field of the simple air/silicon environment, using periodic ports and boundary conditions. The scatterer is then added, and the periodic boundary condition is replaced with a perfectly-matched layer, to solve for the scattered field. This simulation should yield the scattered field, albeit with the condition that each scatterer is distant enough from neighboring scatterers to ignore mutual coupling. We also performed identical simulations using periodic boundary conditions. The mesh was chosen automatically by the software, except for the region containing and immediately adjacent to the scatterer, where we used a highly compressed mesh on the advice of several technicians.

A sample scatterer and the resultant visualization of the cross scattered field is shown in Figure 4.

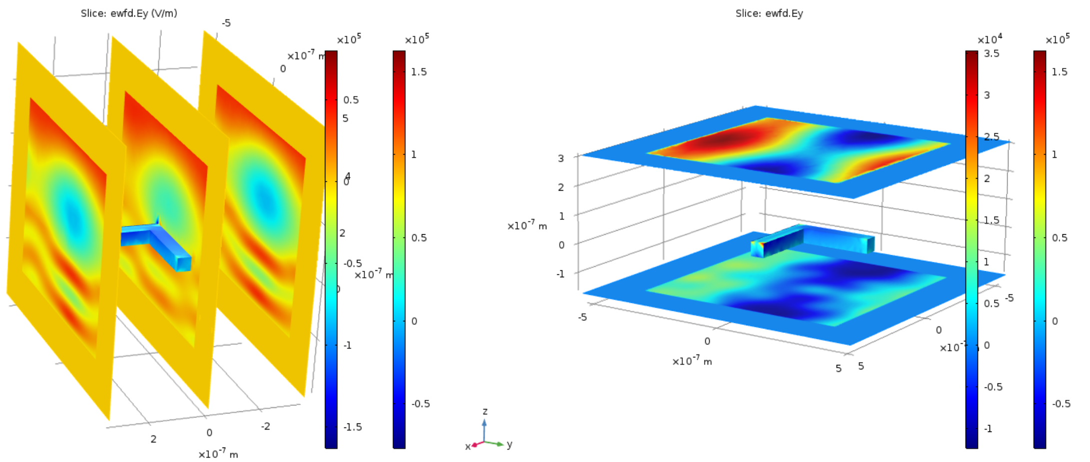

Figure 4 Slices of the y-component of the electric field for a two armed plasmonic scatterer (with a 90° bend) subjected to a TE x-polarized electric field.

After simulation, the electric field for the above model propagated into the far-field using COMSOL, which uses the Stratton-Chu formulation. The phase and intensity are easily extracted from COMSOL as Arg($E_{scat, y}$) and Mag($E_{scat, y}$). A sample plot and list of resultant data for arbitrary parameters can be found in the Appendix. As elaborated on in the fabrication section, due to incomplete fabrication, we were unable to examine individual scatterers to determine their physical characteristics and narrow down on a desired width/height. As a result, the length/angle data for a fixed height and width is rather sparse, due to much of the data being for additional widths/heights.

Fabrication

Our fabrication process consists of a few relatively straightforward steps. We began with a bare, mechanical grade Si wafer with native oxide. The wafer is cleaned with acetone and IPA to remove any dirt or dust from the surface. The wafer is then primed with hexamethyldisilazane (HMDS) vapor in the YES 1224P HMDS/IR Oven to promote adhesion of the photoresist to the wafer surface. HMDS promotes photoresist bonding to the wafer surface while simultaneously providing a hydrophobic coating. After HMDS vapor priming, the electron beam photoresist (ZEP520A) is spun onto the wafer for 60s at 6000 RPM to create a 305nm thickness resist layer. The wafer is then prepared for the electron beam lithography (EBL) process, where a dose of 85 microC/cm^2 is applied to the resist for full exposure. The patterns are defined in a .gds design file prepared in LayouEditor to define shapes, and in BEAMER software to apply appropriate doses and corrections around sensitive features. After all doses and patterns are clearly defined in software, the output file is input into the Elionix ELS-7500EX E-beam Lithographer tool. The resist is subsequently developed in o-xylene to remove exposed resist and rinsed in IPA to ensure removal of any remaining particulates.

To make our gold scatterers, we then deposit metals via electron beam evaporation using the Lesker PVD75 E-beam evaporator. First we deposit a 5nm-thick adhesion layer of Ti, followed by a 40nm-thick layer of Au to function as our plasmonic material.

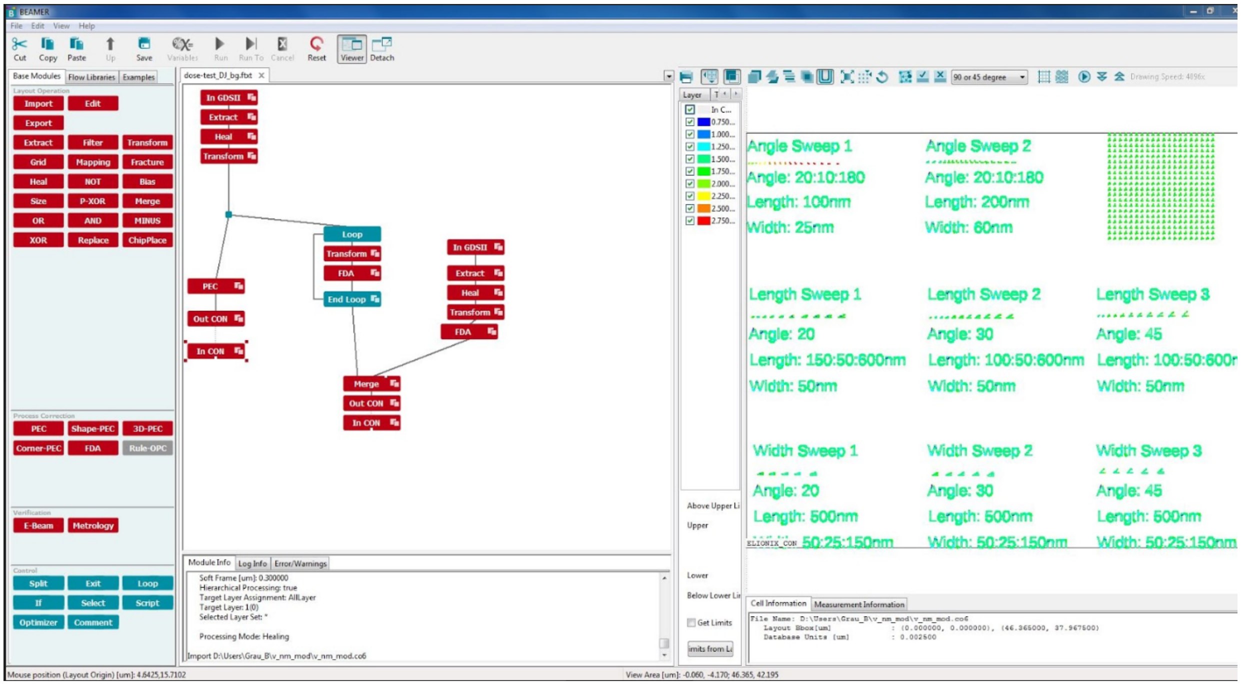

Figure 5 Beamer file showing various sweeps of different parameters, and including a periodic array of a single type of scatterer.

The first objective of our first batch (Figure 5) of fabrication run was to sweep through a variety of parameters in order to determine what feature size was feasible. Due to the impact that any non-idealities would have on the resonances of the plasmonic scatterers, our goal for our first run was primarily to identify what feature sizes would lead to physical results that were closest to our ideal model, and for any extreme cases, if we would have to make any geometrical adjustments in COMSOL. This was done with the aim of fixing our width/height, since they had the smallest dimension and were most likely to be prone to nonidealities. Our second goal, was to confirm the validity of our simulations, and in particular determine which boundary conditions were most suitable.

During our first round of fabrication, the machine was not functioning and we did not obtain any results. After our second round of fabrication we were able to obtain faint optical images (Figure 6) of our fabricated scatterers. However, despite some effort it was not possible to obtain SEM images. This suggests that either the dosage during exposure was not high enough, or that development did not fully cut through to the silicon. In either case, a thin layer of PMMA on the surface of the scatterer and substrate would have formed, preventing SEM images from being taken. Unfortunately, due to time constraints, it was not possible to perform any further fabrication.

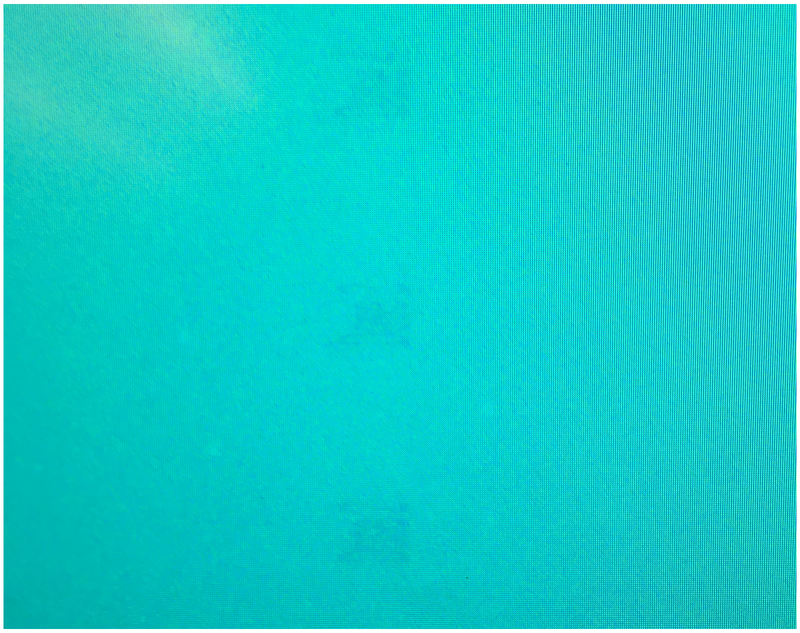
Figure 6 Optical image of fabricated scatterers

Conclusions

Throughout the past year, we have learned a number of lessons pertaining to the theory of Fourier optics and plasmonics as well as the process of building a device. In terms of Fourier optics, we developed a clearer understanding of how a lens produces the Fourier transform, and about the significance of the Fourier transform for optical computing. Through reading literature, we obtained an understanding of how plasmonics could be used to mimic the effect of a lens at the nanoscale. We took this theoretical knowledge and simulated a core component of the meta-surface: a single scatterer. By combining many scatters that produced phase delays to create a phase frontier, we aimed to create a flat metasurface lens.

While our COMSOL simulations appear to have worked, we unfortunately ran into a roadblock around fabrication time. While we were unfortunate to run into a few mishaps like the machine failure on our first fabrication attempt, given that the fabrication facility has a large backlog of projects and training times are quite unpredictable, starting earlier in our engagement with the QNF would have been wise. However, despite being unable to see the project to completion, we found this experience invaluable in teaching us about the principles of optics and plasmonics, and in gaining practical fabrication experience.

References

1. Grote, R. R., Huang, T. Y., Mann, S. A., Hopper, D. A., Exarhos, A. L., Lopez, G. G., ... & Bassett, L. C. Imaging a nitrogen-vacancy center with a diamond immersion metalens. *arXiv preprint arXiv:1711.00901*. (2017).
2. Gorlach, M. A., Ni, X., Smirnova, D. A., Korobkin, D., Zhirihin, D., Slobozhanyuk, A. P., ... & Khanikaev, A. B. Far-field probing of leaky topological states in all-dielectric metasurfaces. *Nature communications*, **9**, 909 (2018).
3. Hong, L., Li, H., Yang, H., & Sengupta, K. Nano-plasmonics and electronics co-integration in CMOS enabling a pill-sized multiplexed fluorescence microarray system. *Biomedical optics express*, **9**, 5735-5758 (2018).

4. Estakhri, N. M., Edwards, B., & Engheta, N. (2019). Inverse-designed metastructures that solve equations. *Science*, **363**, 1333-1338 (2019).
5. azeem. When Moore's Law Met AI – Artificial Intelligence and the Future of Computing. *Medium* (2017). Available at: https://medium.com/s/ai-and-the-future-of-computing/when-moores-law-met-ai-f572585da1b7. (Accessed: 16th November 2018)
6. Caulfield, H. J. & Dolev, S. Why future supercomputing requires optics. *Nat. Photonics* **4**, 261–263 (2010).
7. Rareshide, M. Power in the Data Center and its Cost Across the U.S. Available at: https://info.siteselectiongroup.com/blog/power-in-the-data-center-and-its-costs-across-the-united-states. (Accessed: 16th November 2018)
8. Shah, A. HPE looks to move data between computers at the speed of light. *Computerworld* (2016). Available at: https://www.computerworld.com/article/3085219/high-performance-computing/hpe-looks-to-move-data-between-computers-at-the-speed-of-light.html. (Accessed: 16th November 2018)
9. Hardesty, L. Selling chip makers on optical computing. *MIT News* Available at: http://news.mit.edu/2009/optical-computing. (Accessed: 16th November 2018)
10. WSTS, & SIA. Global semiconductor industry market size 1987-2019 | Statistic. *Statista - The Statistics Portal* Available at: https://www.statista.com/statistics/266973/global-semiconductor-sales-since-1988/. (Accessed: 16th November 2018)
11. Naeher, U., Suzuki, S. & Wiseman, B. *The evolution of business models in a disrupted value chain*. (2011).
12. Yu, N. *et al.* Light Propagation with Phase Discontinuities: Generalized Laws of Reflection and Refraction. *Science* **334**, 333–337 (2011).
13. Kats, M. A., Genevet, P., Aoust, G., Yu, N., Blanchard, R., Aieta, F., ... & Capasso, F.. Giant birefringence in optical antenna arrays with widely tailorable optical anisotropy. *Proceedings of the National Academy of Sciences*, **109**, 12364-12368 (2012).
14. Aieta, F. *et al.* Aberration-Free Ultrathin Flat Lenses and Axicons at Telecom Wavelengths Based on Plasmonic Metasurfaces. *Nano Lett.* **12**, 4932–4936 (2012).

Appendix

For fixed h = 50nm, t = 40nm, λ = 2μm

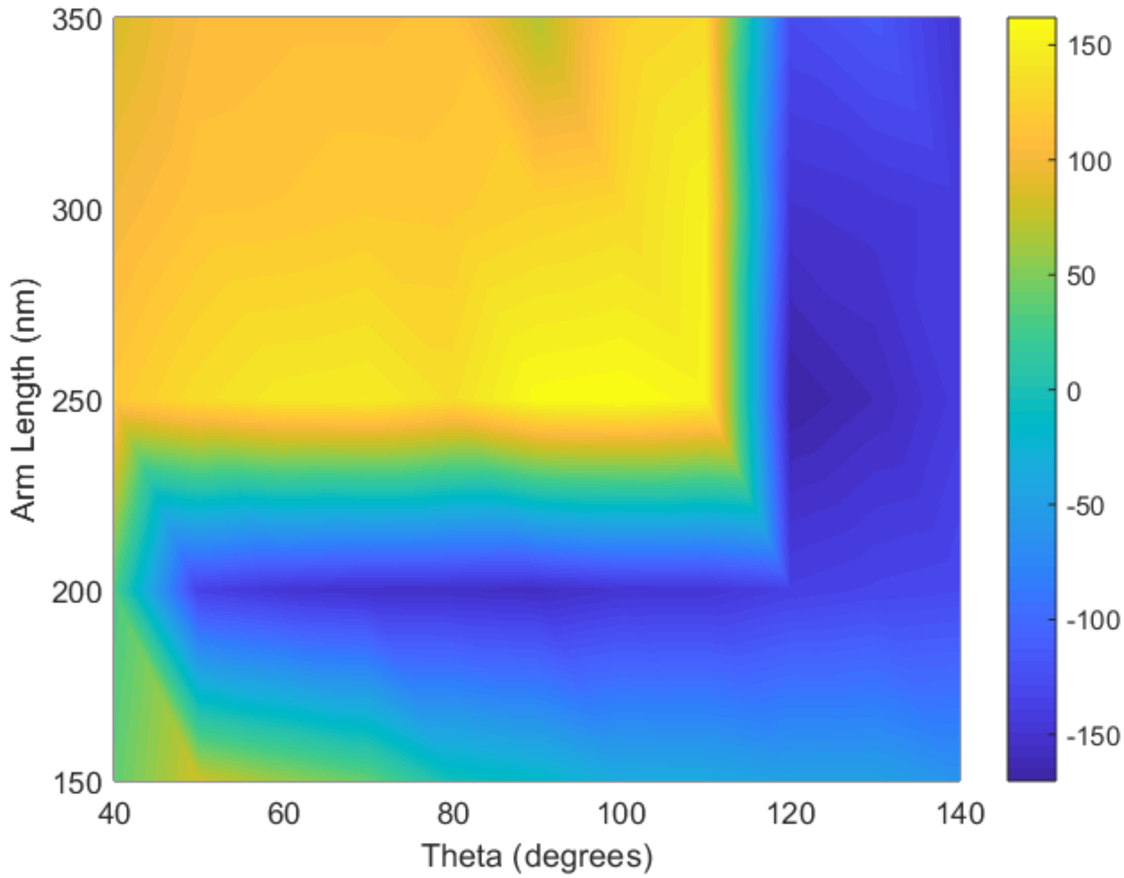

Figure 7 Plot of scattered light phase (in degrees) for listed parameters

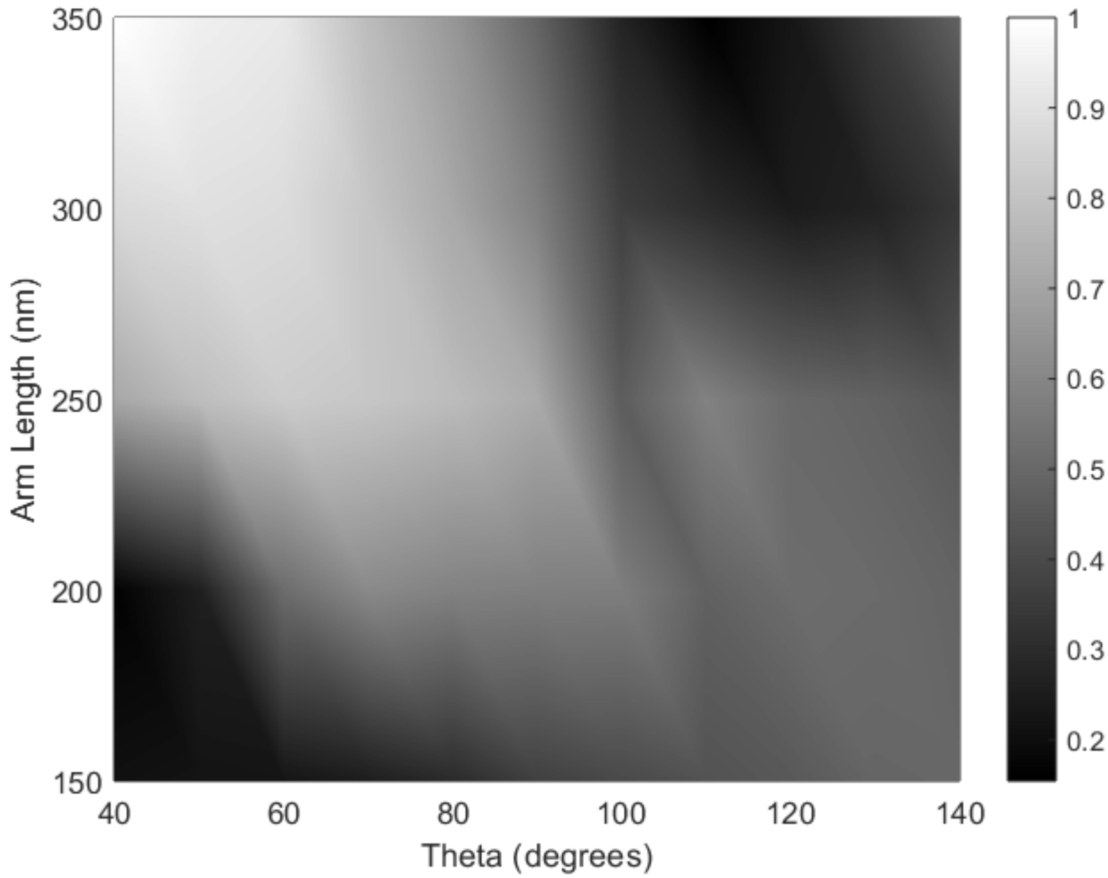

Figure 8 Plot of scattered light normalized intensity for listed parameters

l (nm)	θ (º)	phase delay (º)	intensity (normalized)
150	40	38.72	0.209
200	40	28.82	0.163
250	40	117.48	0.708
300	40	100.32	0.874
350	40	85.36	1.000
150	50	80.08	0.220
200	50	-137.06	0.259
250	50	134.2	0.782
300	50	114.18	0.896
350	50	104.94	0.948
150	60	58.96	0.225
200	60	-148.5	0.516
250	60	144.32	0.830
300	60	115.72	0.882
350	60	108.46	0.926
150	70	40.04	0.254

200	70	-153.56	0.612
250	70	146.74	0.812
300	70	119.68	0.808
350	70	108.46	0.778
150	80	-3.96	0.298
200	80	-154.44	0.586
250	80	134.86	0.778
300	80	118.8	0.712
350	80	111.98	0.656
150	90	-15.18	0.368
200	90	-157.19	0.577
250	90	159.5	0.721
300	90	125.62	0.580
350	90	68.86	0.486
150	100	-34.98	0.398
200	100	-149.16	0.572
250	100	161.92	0.463
300	100	130.24	0.363
350	100	123.86	0.272
150	110	-37.84	0.429
200	110	-147.928	0.477
250	110	153.78	0.586
300	110	152.02	0.301
350	110	131.56	0.154
150	120	-46.86	0.448
200	120	-137.94	0.516
250	120	-170.28	0.503
300	120	-150.26	0.246
350	120	-128.04	0.229
150	130	-47.96	0.490
200	130	-132.66	0.508
250	130	-159.72	0.481
300	130	-146.74	0.268
350	130	-115.72	0.350
150	140	-61.16	0.494
200	140	-129.36	0.486
250	140	-141.68	0.442
300	140	-141.9	0.341
350	140	-148.72	0.479